VARIATION OF TEMPARATURE, PRESSURE, POTENTIAL AND CURRENT DENSITY IN COLD METAL TRANSFER (CMT) WELDING PROCESS

G Prakasham[1], D V Ramana Reddy[2], R Ravi Kumar[3], A Gnan Reddy[4], M Bhargava Chandra[5]
[1] Assistant Professor, [2]Associate professor, [3, 4, 5] Assistant Professor
[1,3,4,5] Department of Mechanical Engineering,
Maturi Venkata Subba Rao (MVSR) Engineering College, Hyderabad, India
[2]Vardhaman College of Engineering

Abstract : A unified comprehensive mathematical model was developed to simulate the transport phenomena occurring in the cold metal transfer welding process (CMT). It includes the arc plasma, droplet generation, velocity, current density, Temperature distribution, onto the workpiece. The continuum formulation is used for the conservation equations of mass, momentum, and energy in the arc plasma region. The distribution of pressure, temperature, and flux for the plasma zone are all calculated as a function of time. It is also observed that these distributions for a moving heat source are non-axisymmetric and the peaks shift to the arc moving direction. It is observed that the temperature obtained in the Cold metal transfer welding process is less than the conventional welding methods like GMAW, GTAW, SMAW, and SAW.

Index Terms -Cold metal transfer welding; Gas metal arc welding; Temperature; Potential; Pressure; Current density

I. INTRODUCTION

Less than a decade ago, Fronius began to develop and introduce a new metal inert gas (MIG)/metal active gas (MAG) dip-transfer arc process called cold metal transfer (CMT), in which the welding process is defined by the cyclic alternations between arcing and short circuiting phases. According to the invention, during the arc phase, welding consumable is displaced toward the workpiece until it makes contact with the weld piece and during the short-circuit phase the welding consumable displacement is reversed and the consumable is then moved away from the workpiece. The welding current and voltage are controlled during the arc phase in a way that the welding consumable melts and forms a droplet. During the short-circuiting phase, the droplet bridges the gap between the electrode and the workpiece and while the control system reciprocates the wire feeding, the droplet launches to the weld pool when there is no arc driven by the surface tension (cold transfer).When comparing with any other fusion welding process cold metal transfer welding is having many advantages like spatter free, less power consumption, fine droplet etc.

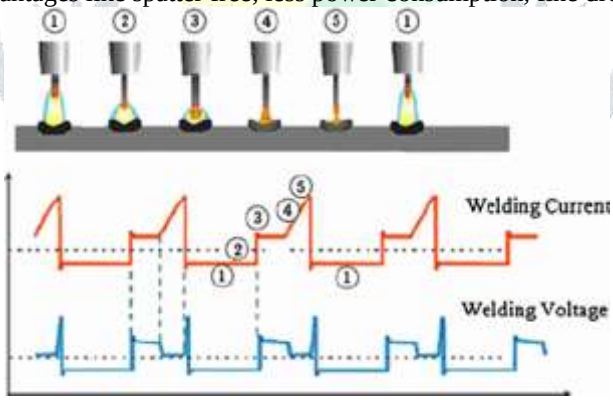

Fig 1. Metal Transfer Process, Current and Voltage Waveforms of Cold Metal Transfer Welding

The modeling of electric arc began at 1935 with Elenbaas et al. [6] and Heller et al. [8]. In their models, they solved the energy conservation equation by considering Joule heating as a source of energy and conduction as the main mechanism for heat transfer. In 1955 Marcker et al. [9] considered the electromagnetic force and pressure gradient and derived a model for the arc. By solving the flow and continuity equations analytically, he obtained an approximate value for the maximum pressure. As reported by Boulos et al. [6] in 1967, Watson and Pegot [10], for the first time combined flow and energy equations in a two-dimensional model and through solving these equations numerically obtained accurate results for flow and temperature fields. Their model considered only the column of the arc. Zhu et al. [14] combined both arc and cathode by using a one dimensional model for the electrode layer [15]. They divided the calculation domain into three parts electrode (cathode) cathode sheath and arc column. By defining two internal boundaries between these parts they solved the relevant conservation equations for the electrode and the arc. The results of this model are in fairly good agreement with some available experimental data. Modeling of the arc in the GMAW process has only started recently and it will be sometime before the appearance of a well-developed model. Some of important areas to study for GMAW can be listed as follows:

- Non-thermionic cathode nature and behaviour in different arises.
- Effect of composition of gas on the arc properties.
- Consumable-arc interaction.
- Droplet-arc interaction

II. MODEL DEVELOPMENT OF COLD METAL TRANSFER WELDING

A schematic sketch of a DCEP gas metal arc welding is illustrated in Figure 2.1.The DCEP configuration is preferred in the GMAW process because of the melting of the continuously fed electrode. For this reason the work piece is the cathode. Electrons, either emitted from the cathode (work piece) or produced in the arc, condense on the anode (electrode). The heat transferred by the electrons dong with the radiation heat and more importantly the Joule heating into the electrode raise the temperature of the electrode to the melting point The heat content of the falling droplets will be transferred to the weld pool. Other heat sources for the work piece will be radiation and convection.

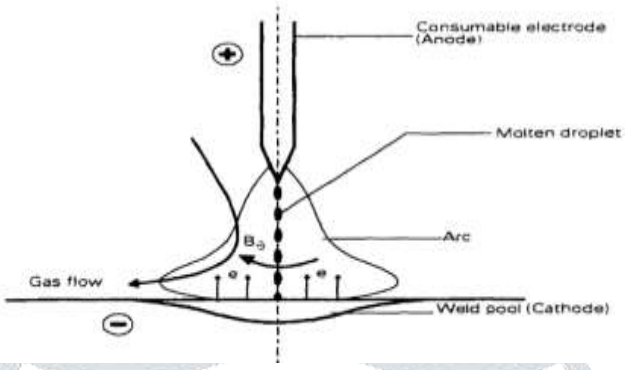

Fig 2 Schematic of Welding Arc (GMAW)

III. GOVERNING EQUATIONS:

In the GMAW process, there are electrons emitted from the cathode which pass through the gap between the work piece and the wire electrode to condense on the anode (wire electrode). The interaction of the magnetic field produced by this current with the current itself produces an electromagnetic force which is the main driving force for the plasma. This phenomenon is very similar to the case in the GTAW process. Although in the GMAW, the electron current direction is opposite to that of the GTAW, the change in the sign of the magnetic field results in the electromagnetic force to act in the same direction as the case of the GTAW. The thermal effect of the electric current which originates from the Joule heating, keeps the temperature high enough for maintaining stable plasma.

Conservation of mass:

$$\partial P/\partial t + \partial/\partial x(\rho u) + \partial/\partial y(\rho v) = 0$$

Conservation of axial momentum in Y-direction:

$$\partial(\rho v^2)/\partial y + \partial(\rho uv)/\partial x = -\partial P/\partial y + 2\partial(\mu \partial v/\partial y)/\partial y + \partial(\mu(\partial v/\partial x + \partial u/\partial x)/\partial x) + J_y B_y$$

Continuity of current: (in terms of potential)

$$\frac{\partial^2 \phi}{\partial x^2} + \frac{\partial^2 \phi}{\partial y^2} = 0$$

Since the arc is axi-symmetric, the azimuthal component of the magnetic field will be the only component that acts on the plasma through the Lorentz force. The azimuthal component of the magnetic field can be calculated by following relation from Ampere's Law.

Maxwell's equation:

$$B_\theta = \frac{\mu_0}{r} \int_0^r J_z r\, dr$$

Conservation of Energy:

$$\frac{\partial \rho u h}{\partial z} + \frac{1}{r}\frac{\partial \rho r v h}{\partial r} = \frac{\partial}{\partial z}\left(\frac{k}{C_p}\frac{\partial h}{\partial z}\right) + \frac{1}{r}\frac{\partial}{\partial r}\left(\frac{k}{C_p} r \frac{\partial h}{\partial r}\right) + \frac{J_z^2 + J_r^2}{\sigma} + \frac{5k_b}{2e}\left(\frac{J_z}{C_p}\frac{\partial h}{\partial z} + \frac{J_r}{C_p}\frac{\partial h}{\partial r}\right)$$

A non-uniform grid point system is employed with finer grid sizes near the consumable electrode. The distance between the electrodes is varied from 2.0 to 10.0 mm. The inflow boundary at the top of the domain is taken at 20.0 mm above the electrode face (anode surface). The boundary at the side is 20.0 mm away from die axis of symmetry. The corresponding boundary conditions are given in Table 4.1.In here the shielding gas flow is also considered since phenomenon such as convection and radiation are predominant to obtain the flux value. The domain is divided as such for better understanding in different sections of arc plasma and around it. It is also done for ease in solving the equations.

	BC[1]	CD[1]	DE	EF	FG	GH	HB
v	0	$\frac{\partial \rho r v}{\partial r} = 0$	0	0	0	0	0
u	u= constant	$\frac{\partial u}{\partial r} = 0$	0	0	$\frac{\partial u}{\partial r} = 0$	0	0
H	T=500K	Inflow: T=1000K Outflow: $\frac{\partial h}{\partial r} = 0$	T=500K	$T=T_{m,wp}$	$\frac{\partial h}{\partial r} = 0$	$T=T_{m,elec}$	$T=T_{m,elec}$
Φ	$\frac{\partial \emptyset}{\partial z} = 0$	$\frac{\partial \emptyset}{\partial r} = 0$	$J_c=0$	$J_c = 1/\pi R_c^2$	$\frac{\partial \emptyset}{\partial r} = 0$	$-\sigma \frac{\partial \emptyset}{\partial z} = 1/\pi R_c^2$	$-\sigma \frac{\partial \emptyset}{\partial z} = 1/\pi R_c^2$

IV. ASSUMPTIONS:

- Density is constant with respect to temperature and time in arc region.
- Thermal conductivity is constant in arc.
- Radiation losses in arc region are neglected.
- Since the droplet spends only a very short time in flight it is assumed that there is no droplet between the consumable electrode and the work piece. The short life of the droplet in the very high temperature zone combined with the high velocity of the plasma about the axis of symmetry lead to the assumption that there is no metal vapor in the space between the electrodes. A limited amount of metal vapor enters the plasma but it cm not diffuse radially into the outer parts. Therefore a small amount of metal vapor is present near the axis of symmetry, very close to the droplets, but the effect of this on the whole arc is insignificant.
- It is assumed that the arc is axially symmetric so that the equations can be written in two-dimensional cylindrical coordinates.
- Laminar flow is assumed. This assumption is justified by McKelliget and Szekely et al. [8] on the basis of laminar-turbulent transition for a free jet.

Pressure Calculations Due To Weld Droplet In The Arc Region:

Conservation of mass:

$$\partial P/\partial t + \partial/\partial x(\rho u) + \partial/\partial y(\rho v) = 0$$

Assuming the weld metal transformation to be **Globular** mode of transfer (gravity plays the major role)

$$v = \sqrt{2g(h-y))}$$
$$\partial v/\partial y + \partial u/\partial x = 0$$
$$\partial \sqrt{2g(h-y))}/\partial y + \partial u/\partial x = 0$$
$$\partial \sqrt{2g(h-y))}/\partial y + \partial u/\partial x = 0$$

On solving:

$$u = \frac{\sqrt{g} * x}{\sqrt{2(h-y)}} + k$$

Substituting boundary conditions- u=0 at x=0;

$$u = \frac{\sqrt{g} * x}{\sqrt{2(h-y)}}$$

Conservation of axial momentum: Y-axis

$$\partial(\rho v^2)/\partial y + \partial(\rho uv)/\partial x = -\partial P/\partial y + 2\partial(\mu \partial v/\partial y)/\partial y + \partial(\mu(\partial v/\partial x + \partial u/\partial x))/\partial x) + J_y B_y$$

$$\partial(\rho \sqrt{2g(h-y)}^2)/\partial y = \partial(\rho * 2g(h-y)))/\partial y = 2\rho g(0-1)) = -2\rho g$$

$$\partial(\rho uv)/\partial x = \partial/\partial x(\rho * \frac{\sqrt{g}*x}{\sqrt{2(h-y))}} * \sqrt{2g(h-y)})) = \partial/\partial x(\rho g x) = \rho g$$

Now: $2 * \partial/\partial y(\mu \partial v/\partial y)$

Assume Viscosity to be constant

$$2 * \mu\sqrt{2g} * \partial/\partial y(\partial/\partial y(\sqrt{h-y}))$$

On solving:

$$= \frac{-\sqrt{2g} * \mu * (h-y)^{\frac{-3}{2}}}{2}$$

$$\partial/\partial x(\mu(\partial/\partial x(\sqrt{2g(h-y)}) + \partial/\partial y(\frac{\sqrt{g} * x}{\sqrt{2(h-y)}}))$$

On solving:

$$\frac{\mu * \sqrt{g}}{2\sqrt{2}} * (h-y)^{\frac{-3}{2}}$$

Now: $1+2 = -\partial P/\partial y + 3 + 4 + T_B$

$$-\rho g = -\partial P/\partial y + J_B - (h-y)^{\frac{-3}{2}} * \frac{\sqrt{g} * \mu}{2\sqrt{2}}$$

Integrating with respect to 'y' and substituting boundary condition: at y=h, P=0

$$P = \rho g y + J_B + \frac{\mu\sqrt{g} * (h-y)^{\frac{-1}{2}}}{\sqrt{2}} - \rho g h - J_B h$$

Similarly about x-direction

$$P = \frac{-\rho g x^2}{2(h-y)} - J_B x + \frac{3\mu\sqrt{g} * x^2 (h-y))^{\frac{-5}{2}}}{8\sqrt{2}}$$

Fluid surface is subjected to surface tension because of molecular forces at the surfaces change abruptly as the fluid properties change discontinuously. It is expressed as

$P_s = \gamma k$

Where γ - surface tension coefficient

And $k = -(\bigtriangledown(\frac{\vec{n}}{|\vec{n}|})) = \frac{1}{|\vec{n}|} * (\frac{\vec{n}}{|\vec{n}|}) * \bigtriangledown - (\bigtriangledown * \vec{n})$

Considering sphere surface equation:

$x^2 + y^2 + z^2 = k$ And obtaining the value of $\bigtriangledown\vec{n}/|\vec{n}|$

We get

$\bigtriangledown\vec{n}/|\vec{n}| =$

$(\vec{i}/\sqrt{2yh + m - h^2}) + (\vec{j}(2yh + m - h^2 - yh)/(2yh + m - h^2) * \sqrt{2yh + m - h^2}))$

Adding the above surface tension term to pressure equation and solving the final equation in MATLAB.

Calculation of Potential, Temperature and Flux due to electrode droplet on the work piece surface:

For calculating Potential:

Current continuity equation:

$$\frac{\partial^2\phi}{\partial x^2} + \frac{\partial^2\phi}{\partial y^2} = 0$$

Current continuity:

$$\frac{1}{r} * \frac{\partial}{\partial r} r \frac{\partial\phi}{\partial r} + \frac{\partial^2\phi}{\partial z^2} = 0$$

Ohm's law:

$$J_r = -\sigma_e \frac{\partial\phi}{\partial r}, J_z = -\sigma_e \frac{\partial\phi}{\partial z}$$

On solving the above equations and applying boundary conditions

$$\phi = cos(\frac{\pi y}{0.01}) cos(\frac{\pi x}{0.01})$$

For calculating Temperature:

The heat source models that are available are double ellipsoidal, Gaussian, hyperboloid and paraboloid, on substituting the assumed boundary conditions into the above mentioned heat source model, double ellipsoidal model was the one that gave better result. The equation considered is

$$T = 1000 - (\frac{(7 * 10^5 * y + 1000) * x^2}{h^2}) + (7 * 10^5 * y + 1000)$$

For calculating Flux:

$$Q = \sigma * ((T^4 - T_{atm}^4) + h(T - T_{atm}))$$

$$Q = 5.67 * 10^{-8}(T^4 + 10 * (T))$$

In real world welding, the arc is moving, the weld pool is non axi-symmetric, and the heat flux at the work piece are greatly affected by the weld pool shape. In addition, the geometries of many weld joints such as T-joint, lap joint, corner joint, are naturally three-dimensional.

Finally, perturbations such as external magnetic field may deflect axi-symmetric plasma arc from its axi-symmetry. A 3D model is necessary to investigate all these applications. Using MATLAB software 3D model of following entities were found.

Governing equation for variation in shielding gas velocity at nozzle:

$$v(r) = \frac{2Q}{\pi} \frac{\left\{R_n^2 - r^2 + (R_n^2 - R_w^2)\frac{\ln(r/R_n)}{\ln(R_n/R_w)}\right\}}{\left\{R_n^4 - R_w^4 + \frac{(R_n^2 - R_w^2)^2}{\ln(R_n/R_w)}\right\}} + V_w \frac{\ln\frac{R_n}{r}}{\ln\frac{R_n}{R_w}}$$

V. RESULTS AND DISCUSSION

Variation In Velocity Of Shielding Gas At Nozzle:

```
x=0.001:0.0001:0.01;
z=(4.5.*10.^(-2)).*(log(x.\0.01));
a=(0.122.*10.^(5));
b=0.0001-(x.*x)+((0.0001-0.000001).*(2.3026.\(log(0.01.\x))));
c=a.*b;
d=c+z;
figure
plot(x,d)
```

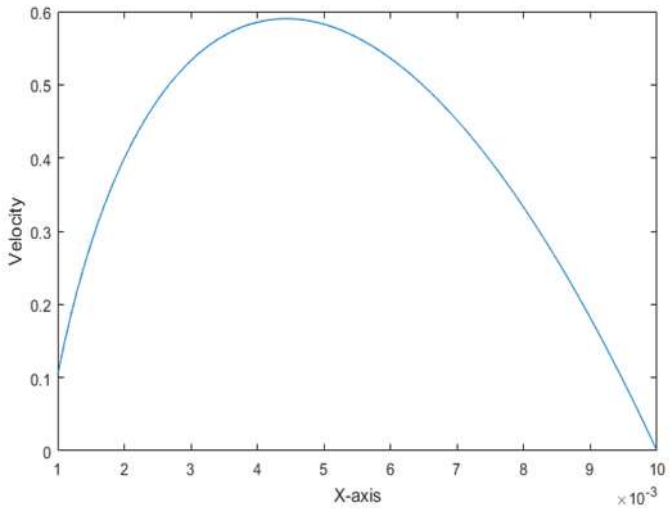

FIG 3. Variation of Velocity of Shielding Gas at Nozzle

Pressure In The Arc Region As A Function Of F(X, Y):

```
x=-0.01:0.004:0.01;
y=0:0.001:0.009;
[X,Y]=meshgrid(x,y);
Z=(((37670.25).*(X.^2)).\(Y-0.01))+((0.08305).*(X.^2)).\((0.01-Y).^2.5)-(X);
Figure
surf(X,Y,Z)
```

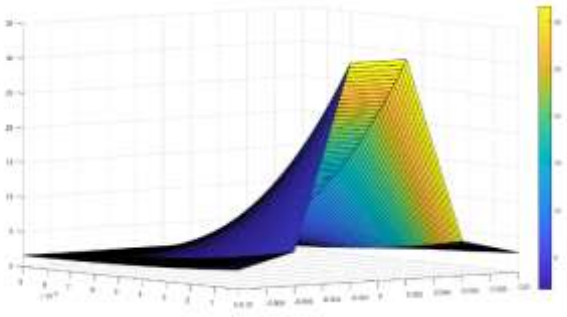

Fig 4. Pressure Variations Due To Electrode Droplet In Arc Column

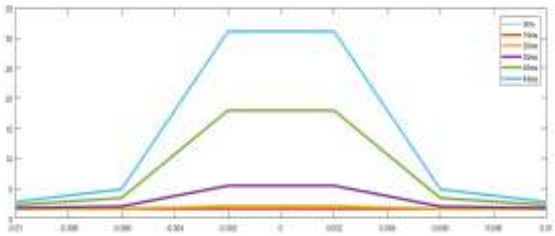

Fig 5. Pressure Variations In Arc Column At Different Time Intervals

Variation of Current Density in Arc Region:

```
x=0:0.0001:0.01;
y=0:0.0001:0.01;
[X,Y]=meshgrid(x,y);
a=((2.71.^(152.33.*Y))-(2.71.^(-(52.33.*Y))));
c=((0.06.\X));
b=sin(pi.*c);
e=(99.089.*10.^(5)).*b.*a;
d=((2.71.^(152.33.*Y))+(2.71.^(-(52.33.*Y)))).*cos(pi.*c).*(99.089.*10.^(5));
z=d+e;
figure
surf(X,Y,d)
```

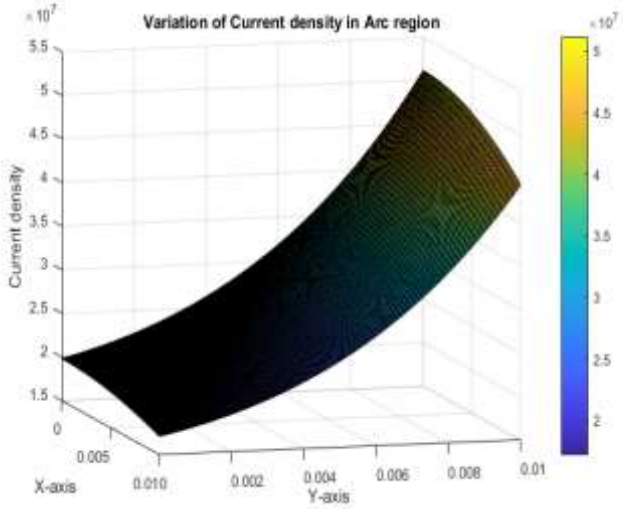

Fig 6. Variation of Current Density in Arc Region

Potential Variation In Arc Region

```
x=0:0.001:0.03;
y=0:0.001:0.03;
[X,Y]=meshgrid(x,y);
a=((2.71.^(152.33.*Y))-(2.71.^(-(52.33.*Y))));
c=((0.06.\X));
b=cos(pi.*c);
z=0.2459.*(a).*(b);
figure
surf(X,Y,z)
```

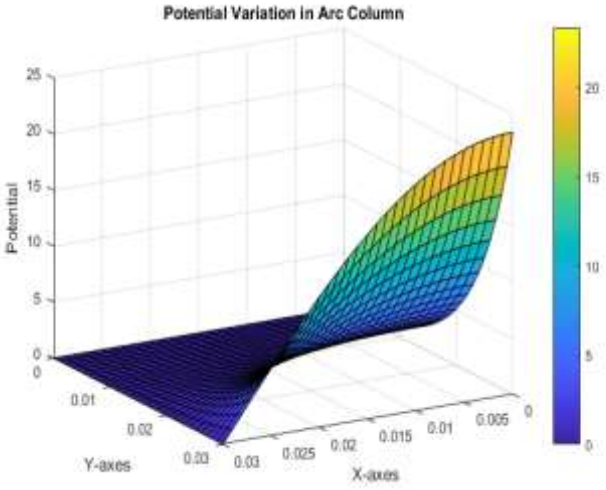

Fig 7. Potential Variations Due To Electrode Droplet In Arc Region

Temperature On The Work Piece Surface As A Function Of F(X, Y):

$$T = 1000 - (\frac{(7 * 10^5 * y + 1000) * x^2}{h^2}) + (7 * 10^5 * y + 1000)$$

The above governing equation is used for 3D model Generation in MATLAB.

```
x=-0.01:0.0004:0.01;
y=0:0.0001:0.01;
[X,Y]=meshgrid(x,y);
z=(1000-((7.*10.^5.*Y)+1000)).*(0.01.^(-2)).*(X.^2)+((7.*10.^5.*Y)+1000);
figure
surf(X,Y,z)
```

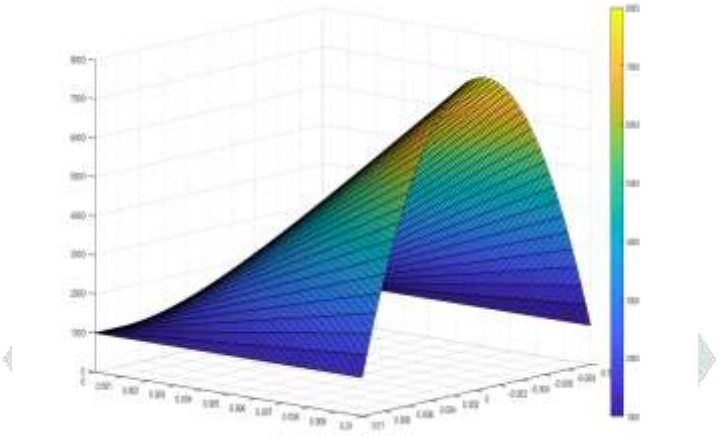

Fig 8. Temperature Variations Due To Electrode Droplet On The Work Piece Surface

For Flux On The Work Piece Surface As A Function Of F(X, Y)

$$Q = 5.67 * 10^{-8}(T^4 + 10 * (T))$$

The above governing equation is used for 3D model Generation in MATLAB.

```
x=-0.01:.0004:.01;
y=0:.0001:0.01;
[X,Y]=meshgrid(x,y);
z=(1000-((7.*10.^5.*Y)+1000)).*(0.01.^(-2)).*(X.^2)+((7.*10.^5.*Y)+1000);
XX=((5.67.*10.^(-8)).*(z.^4)+(10.*(z)));
figure
surf(X,Y,XX)
```

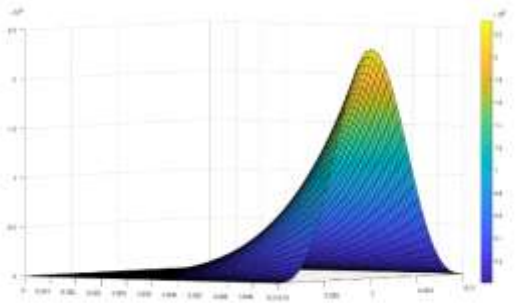

Fig 9. Flux Variations Due To Electrode Droplet On The Work Piece Surface

V. CONCLUSION:

- A 3D Mathematical model for the arc plasma region in GMAW was formulated.
- A 3D Mathematical model for the CMT on work piece was formulated for temperature distribution.
- The current density, velocity, pressure, potential and temperature variation, moving heat source in arc region are calculated as a function of time.
- The distribution of temperature, heat flux, potential on the work piece surface for both GMAW and CMT are obtained by Gaussian distribution.
- On comparing the above results it is observed that the temperature developed in weld pool and heat affected zone is less (about 20%) when compared with conventional welding methods such as GMAW, GTAW, SMAW, SAW.

VI. REFERENCES:

[1] Heat and Mass Transfer in GMAW Part-I by J.Hu, H.L.Tsai.
[2] Three-dimensional modeling of arc plasma and metal transfer in gas metal arc welding by G.Xu, J,Hu, H.L.Tsai.
[3] Computational Weld Mechanics by John.A.Goldak, Mehdi Akhalgi.
[4] E. Pfender, "Electric Arcs and Arc Gas Heaters", in Gaseous Electronics. Vol.1, edited by LM. N. Hirsh and H. J. Oskarn. Academic Press inc.. 1978
[5] M. 1. Boulos, "Modelling of Plasma Processes", in Mat. Res. Soc. Symp. Proc. vol. 30. Elsevier Science Publishing Co. Inc.. 1984
[6] W. Elenbaas, Physics. 1935. 1. p.169. (As cited by Pfender [5] and Boulos [6]
[7] Mathematical Modeling of Gas Tungsten Arc Welding (GTAW) and Gas Metal Arc Welding (GMAW) Processes by Massoud Goodzari.
[8] G. Heller, Physicu. 1935. 6. p. 389. (As cited by Pfender [5] and Boulos [6]
[9] H.Marcker, "Plasmastromungen in Lichtbogen Infolge Eigenmagnetischer Kompression". Zritschnfr jïir Physik. 1955.
[10] V. R. Watson and E. R. Pegot. 1967. NASA, TN. D-4042. (As cited by Boulos [6].
[11] C. W. Chang, T. W. Eagar and J. Szekely, 'The Modelling of Gas Velocity Fields in Welding Arcs", in Welding Institute Conference on Arc Physics and Weld Pool Behaviour, 1979.
[12] K. C. Hsu, K. Etemadi and E. Pfender. "Study of Free-Burning High Intensity Argon Arc". J. Appl. Ph-.. 1983, vol. 54.
[13] P. Zhu, J. J. Lowke and R. Morrow, "A Unified Theory of Free-Burning Arcs, Cathode Sheaths and Cathodes", J. Ph-. D: Appl. Phys., 1992. vol. 25.
[14] R. Morrow and I. J. Lowke, "A One-Dimensional Theory for the Electrode Sheaths of Electric Arcs". J. Phys. D: Appl. Phys., 1993.
[15] P. G. Jonnsson, R. C. Westhoff and J. Szekely, "Arc Characteristics in Gas-Metal Arc Welding of Aluminum Using Argon as the Shielding Gas", J. Appl. Phys-1993.